

## Mediterranean Marine Science

Vol 20, No 3 (2019)



### Evaluating the historical sedimentation patterns in two different Mediterranean deep environments (Sardinia and Sicily Channels)

NOUR EL HOUDA HASSEN, NAFAÂ REGUIGUI, MOHAMED AMINE HELALI, NEZHA MEJJAD, ABDELMOURHIT LAISSAOUI, AZZOUZ BENKDDAD, MONCEF BENMASOUR

doi: [10.12681/mms.19558](https://doi.org/10.12681/mms.19558)

#### To cite this article:

HASSEN, N. E. H., REGUIGUI, N., HELALI, M. A., MEJJAD, N., LAISSAOUI, A., BENKDDAD, A., & BENMASOUR, M. (2019). Evaluating the historical sedimentation patterns in two different Mediterranean deep environments (Sardinia and Sicily Channels). *Mediterranean Marine Science*, 20(3), 542–548. <https://doi.org/10.12681/mms.19558>

## Evaluating the historical sedimentation patterns in two different Mediterranean deep environments (Sardinia and Sicily Channels)

Nour El Houda HASSEN<sup>1</sup>, Nafaâ REGUIGUI<sup>1</sup>, Mohamed Amine HELALI<sup>2</sup>, Nezha MEJJAD<sup>3</sup>,  
Abdelmourhit LAISSAOUI<sup>3</sup>, Azzouz BENKADAD<sup>3</sup> and Moncef BENMANSOUR<sup>3</sup>

<sup>1</sup> National Center of Nuclear Sciences and Technologies, Technopole Sidi Thabet, 2020, Tunisia

<sup>2</sup> Laboratory of Mineral Resources and Environment, Department of Geology, Faculty of Sciences of Tunis, University Tunis El Manar, 2092 El Manar II, Tunis, Tunisia

<sup>3</sup> National Center for Energy, Nuclear Science and Technology (CNESTEN), BP1382, 1001 Rabat, Morocco

Corresponding author: [hassenhourhoda@yahoo.fr](mailto:hassenhourhoda@yahoo.fr)

Handling Editor: Aristomenis KARAGEORGIS

Received: 31 January 2019 ; Accepted: 1 May 2019; Published on line: 2 September 2019

### Abstract

The sediment accumulation rate in the Sardinia and Sicily channels in the central part of the Mediterranean Sea was studied by using natural and fallout radionuclides, <sup>210</sup>Pb and <sup>137</sup>Cs, respectively, in two deep sediment cores. Different sedimentation regimes were identified, indicating substantial differences in accumulation rates and historical patterns. The <sup>210</sup>Pb-derived mean accumulation rate found in the Strait of Sardinia was 0.05 g.cm<sup>-2</sup>.y<sup>-1</sup>, lower than that in Sicily Channel (0.1 g.cm<sup>-2</sup>.y<sup>-1</sup>) suggesting an inverse correlation with water depth. Excess <sup>210</sup>Pb inventories were 24 ± 1 and 6.0 ± 0.4 kBq.m<sup>-2</sup>, while the fluxes to the sediment were 745 ± 31 and 188 ± 11 Bq.m<sup>-2</sup>.y<sup>-1</sup> in Sicily and Sardinia channels, respectively. The use of <sup>137</sup>Cs failed to validate the established chronologies, while its inventories were 450 Bq.m<sup>-2</sup> and 355 Bq.m<sup>-2</sup> in the Sicily and Sardinia channel, respectively.

**Keywords:** Mediterranean Sea; Tunisian coast; <sup>210</sup>Pb and <sup>137</sup>Cs; sediment accumulation rate.

### Introduction

The Mediterranean Sea is a large semi-enclosed body of water that is bordered by 21 different countries belonging to Europe, Africa and Asia. The Strait of Gibraltar is the only connection with the Atlantic Ocean in the west, and the Dardanelles and Suez Canal being the connections with the Black and the Red Sea in the east. Geographically, the Sicilian Channel splits the Mediterranean Sea into two different regions; the Western Basin and the Eastern Basin. The water circulation in the Mediterranean Sea is very complex due to i) several spatial and temporal processes that take place at all scales such as the excess of evaporation over precipitation, adjacent rivers runoff and intense topographic and coastal influences, and ii) the presence of three distinct water masses which flow independently throughout the whole Mediterranean Sea; the surface, the intermediate and the deep waters controlling the general circulation pattern (El-Geziry & Bryden, 2010 ; Waldman *et al.*, 2018).

Several studies have been carried out on radionuclides monitoring in environmental matrices (sediment, water and biota) for understanding their behavior and their use as tracers of marine processes in the Mediterranean

Sea (Laissaoui *et al.*, 2008; Garcia-Orellana *et al.*, 2006; Bressac *et al.*, 2017; Hurtado-Bermúdez *et al.*, 2018, among others). Furthermore, deep sediment dynamics in the Mediterranean Sea have also been a topic of great interest in recent decades. Numerous research works have addressed sedimentation and mixing processes in specific areas and, concurrently, quantified radionuclide inventories and fluxes in the sediment compartment (Zuo *et al.*, 1997; Sanchez-Cabeza, 1999; Miralles *et al.*, 2005 ; Eleftheriou *et al.*, 2018). Most of the contributions were based on studies involving radiometric dating and isotopic fingerprints approaches to establish sediment dynamics and origins.

This work has been carried out within the framework of IAEA technical cooperation projects, aiming at the assessment of marine pollution and study of marine processes. This research was carried out to investigate sedimentation processes over the last few decades in the area of Sardinia and Sicilia Channels, being two different environments, in terms of water and sediment dynamics, within the central Mediterranean Sea. The study sites constitute a key area from a hydrodynamic point of view since water masses are exchanged through these Channels between the Western and Eastern Mediterranean Ba-

sins. Another objective is the assessment of  $^{210}\text{Pb}$ ,  $^{226}\text{Ra}$  and  $^{137}\text{Cs}$  levels,  $^{210}\text{Pb}$  and  $^{137}\text{Cs}$  inventories and  $^{210}\text{Pb}$  fluxes onto the sediment of the study sites. Data were used for radiometric dating of sediment cores to establish the age-depth relationships and sedimentation/accumulation rates.

## Material and Methods

### Sampling and sample analyses

Two sediment cores were collected from the Mediterranean Sea, near Tunisian coast, during a sampling cruise carried out on June 2004 on board of the Algerian research vessel *Mohammed Saddik Benyahia*. The first core (SC-1) of 36 cm length was collected between the northern coast and Sardinia Island at a water depth of 1567 m. The second core (SC-2) of 40 cm length was retrieved from the Strait of Sicily, between the north-eastern Tunisian coast and Sicily Island, at a water depth of 726 m. The cores were collected using an Ocean Instrument box corer (40 cm x 40 cm). Cores data and locations are shown in Figure 1 and Table 1.

The cores were sectioned in slices of 1 or 2 cm thicknesses on board the vessel and frozen to preserve them for subsequent analyses. In the laboratory, the samples were freeze-dried and then gently ground to preserve the naturally occurring particles. Particle size distributions were determined in the homogenized sub-samples using a wet Laser Diffraction equipment (Malvern Mastersizer 2000) using the Hydro 2000G Dispersion Unit. The particle size distribution range is 0.02–2000  $\mu\text{m}$ . About 1 g of sample was introduced in the dispersion unit containing demineralised water, used as dispersant, and then measured after a brief time (10 s) of ultrasound application to disperse any agglomerates. The samples homogeneity was checked by analysing each sample in duplicate, and the results were reproducible.

Total  $^{210}\text{Pb}$  ( $^{210}\text{Pb}_{\text{tot}}$ ) activities were determined by alpha spectrometry by measuring the activity of its daughter

product  $^{210}\text{Po}$  after a chemical separation assuming secular equilibrium between the two isotopes. The method of analysis is as follows: About 1 g of sediment samples were spiked with  $^{209}\text{Po}$  as a recovery tracer and were acid digested (1:5:4 HF + HNO<sub>3</sub> + HCl) in teflon beakers on a hotplate (80°C). The digestate was evaporated to dryness and the digestion residue was converted to a chloride salt by repeated evaporation with 12 M HCl, and then dissolved in 0.5 M HCl in presence of ascorbic acid as a reducing agent for Fe<sup>3+</sup>. (Matthews *et al.*, 2007). Po isotopes were spontaneously deposited on a spinning Ag disc and the activity was measured by  $\alpha$ -spectrometry using ORTEC silicon surface barrier detectors coupled to a PC running under Maestro TM data acquisition software (Hamilton & Smith, 1986; Ebaid & Khater, 2006).

Excess  $^{210}\text{Pb}$  activity was calculated by subtracting supported  $^{210}\text{Pb}$ , assumed to be in equilibrium with  $^{226}\text{Ra}$  activity, on a layer-by layer basis by taking the averaged asymptotic  $^{210}\text{Pb}$  value from each total  $^{210}\text{Pb}$  activity (Brenner *et al.*, 2004). Both approaches lead to similar dating results. According to lead-210 profiles, the atmospherically derived components horizon of  $^{210}\text{Pb}$  in both cores extend to only about 7 cm depth and, therefore only these upper portions of the profiles will be used in ages and accumulation rates calculation.

The constant rate of supply (CRS) model has been applied to establish the age-depth relationships and time-dependent sedimentation/accumulation rates in both sediment cores. This model supposes a constant delivery rate of  $^{210}\text{Pb}$  to the sediment over the time interval covered by the core and no post-deposition particles redistribution.

Radionuclide concentrations ( $^{137}\text{Cs}$  and  $^{226}\text{Ra}$ ) were determined by using a high resolution Broad Energy Germanium (BEGe) gamma spectrometer. Weighed samples were introduced into 75 ml containers and sealed to allow equilibrium of  $^{226}\text{Ra}$  and its decay products. The flasks were stored for more than 21 days and then counted for 24 h each.  $^{226}\text{Ra}$  was obtained from  $^{214}\text{Bi}$  photopeak at 609.3 keV. The self-absorption factor was determined by measuring an  $^{241}\text{Am}$  point source placed over the container filled with sediment and the empty container, as

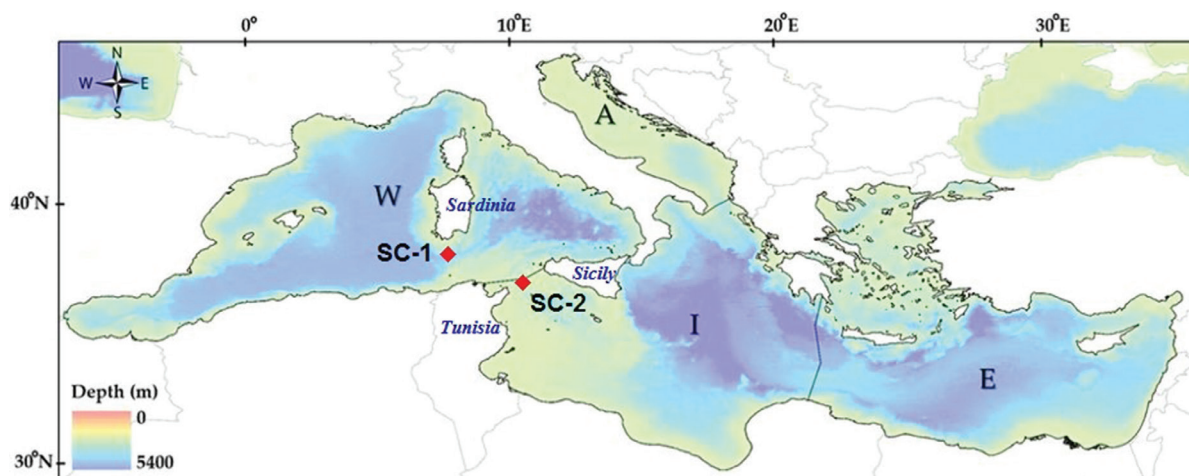


**Fig. 1:** Sampling locations of sediment cores (SC-1 and SC-2) collected from the Mediterranean Sea. The map is showing the bathymetry and the four MSFD areas: Western Mediterranean Sea (W); Adriatic Sea (A); Ionian and Central Mediterranean Sea (I); Aegean and Levantine Sea (E) (Piroddi *et al.*, 2017) (Modified).

**Table 1.** Core location and length, maximum water depth, measured inventories of Excess  $^{210}\text{Pb}$  ( $I^{\text{Pb}}$ ) and  $^{137}\text{Cs}$  ( $I^{\text{Cs}}$ ) and Excess  $^{210}\text{Pb}$  fluxes ( $F^{\text{Pb}}$ ) in tow sediment cores collected from the central part of the Mediterranean Sea.

Core sample	Core length (cm)	Location		Maximum water depth (m)	$I^{\text{Pb}}$ ( $\text{kBq.m}^{-2}$ )	$I^{\text{Cs}}$ ( $\text{Bq.m}^{-2}$ )	$F^{\text{Pb}}$ ( $\text{Bq.m}^{-2}\text{y}^{-1}$ )
		Latitude	Longitude				
SC-1	36	38.132867°	9.064850°	1567	$6.0 \pm 0.4$	450	$188 \pm 11$
SC-2	40	37.608750°	11.495167°	726	$24 \pm 1$	355	$745 \pm 31$

in the procedure used by Khater & Ebaid, 2008. Correction factor for true coincidence summing effect was determined by using a certified reference material, IAEA-327, according to the experimental procedure published by Haddad, 2014. The corresponding sample in the same geometry was measured at two detector-sample distances (0 and 25 cm) to determine activities from the 609 keV peak. At 25 cm, the coincidence summing effect is negligible. Efficiency calibration was carried out for both measurements using a multigamma standard. The reference material IAEA-326 was used for validation. There was good agreement, greater than 95%, between measured and certified values.

## Results and Discussion

### Dating sediment cores

Total  $^{210}\text{Pb}$  and  $^{226}\text{Ra}$  profiles are plotted in Figure 2. Both profiles showed similar patterns; decrease in the first centimeters and then fairly uniform  $^{210}\text{Pb}$  activities downcore with some fluctuations in the SC-1 core. Nevertheless, the activity in the topmost layer of the SC-1 core ( $387 \pm 29 \text{ Bq.kg}^{-1}$ ) is much lower than that of the SC-2 core ( $596 \pm 47 \text{ Bq.kg}^{-1}$ ). A relatively sharp decrease in the activities of the first core can be observed, suggesting different sedimentation rates. The difference in activities in the first layers could be attributed to the grain size difference as shown in the distributions plotted for

both cores (Fig. 3). Indeed, the percentage of sandy particles in the upmost layer of the SC-1 core is 50% versus 30% in the SC-2 core, which could result in enhancing  $^{210}\text{Pb}$  content due to its high affinity to finer particles (Mejjad *et al.*, 2016; Arias-Ortiz *et al.*, 2018; Fontela *et al.*, 2019). The vertical profiles shown in Figure 3 indicate a predominance of mud content and some degree of fluctuations in the upper layers, in particular in the SC-1 core. Below 8 cm depth, both profiles remain quite uniform and practically similar. According to the CRS ages, important amounts of coarse particles were deposited during the last two decades in the area of the sampling point at the Strait of Sicily.

As  $^{210}\text{Pb}$  activity in the sediment is the sum of the supported and the unsupported, or excess, components, the mean activity in the uniform parts of the profiles should correspond to the supported fraction which is, in most cases, in secular equilibrium with  $^{226}\text{Ra}$  activities. These were found to be around  $50.2 \pm 9.6$  and  $46.8 \pm 10.3 \text{ Bq.kg}^{-1}$  throughout the SC-2 and SC-1 cores, respectively. The variability in the two cores reflects disequilibrium between  $^{226}\text{Ra}$  and supported  $^{210}\text{Pb}$  in deep layers of the sediment column. This affects in relatively higher degree the downcore sediment layers which should be too old to be dated by  $^{210}\text{Pb}$  technique.

Results of radiometric dating are given in Figure 4 in which the ages provided by the CRS model are plotted throughout each sediment core. Mass thicknesses was used instead of depth to account for sediment compaction (Abril, 2003; Jia *et al.*, 2018; Bonotto & Garcia-Tenorio,

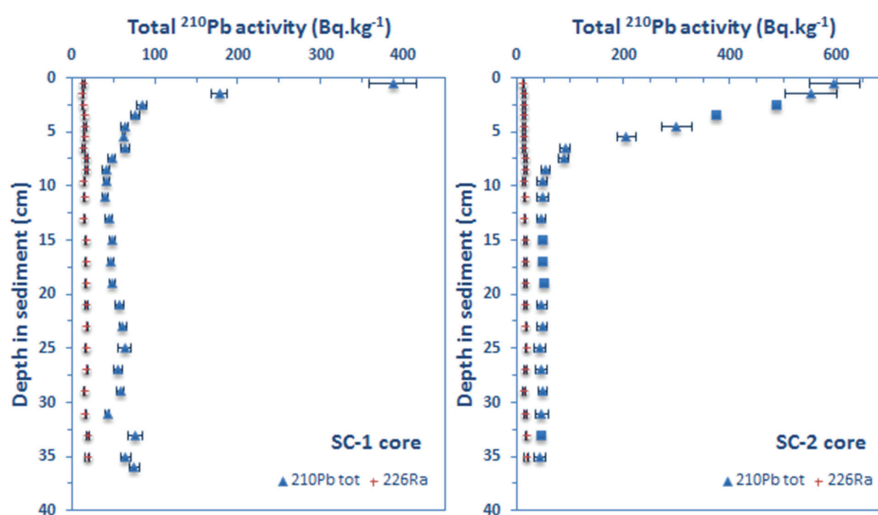


**Fig. 2:** Vertical distributions of total  $^{210}\text{Pb}$  and  $^{226}\text{Ra}$  activities in sediment cores collected from the Mediterranean Sea. (For SC-2, squares represent values obtained by linear interpolation between the measurement points).



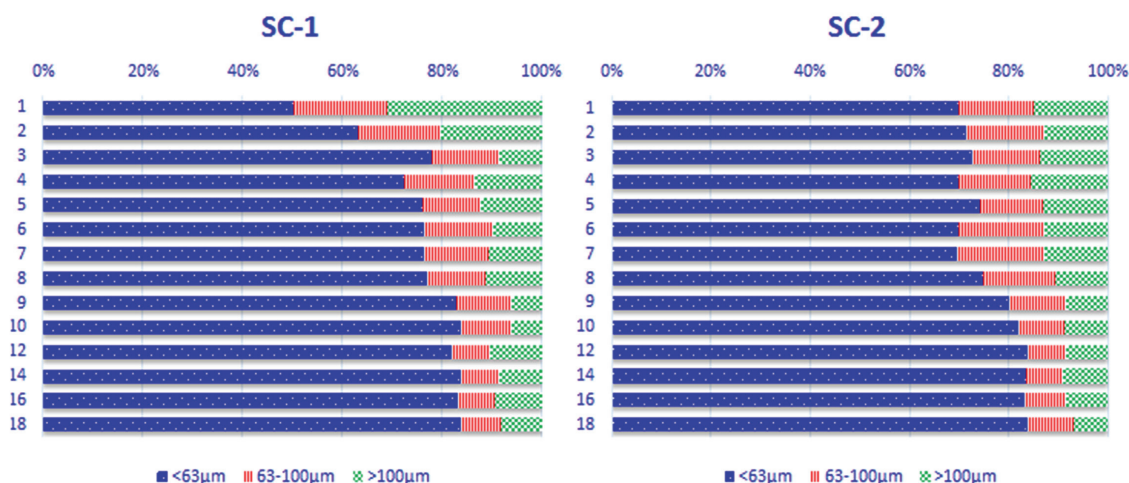


**Fig. 3:** Particle size distributions in SC-1 and SC-2 cores.

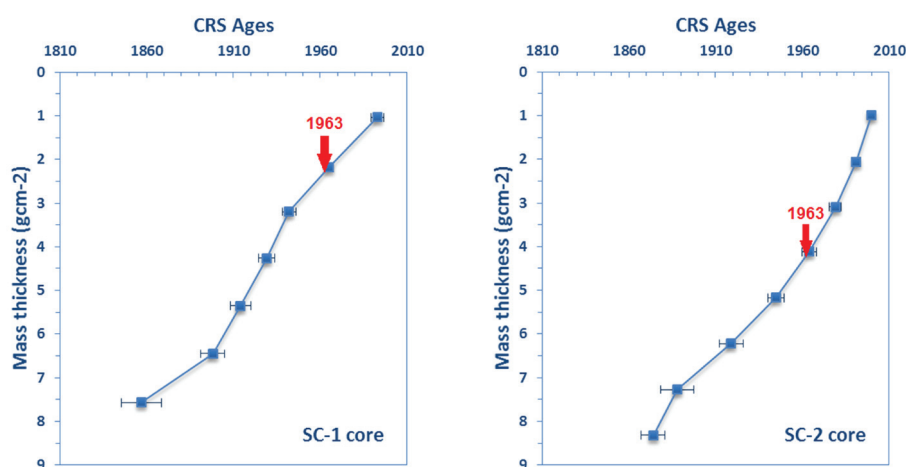


**Fig. 4:** Profiles of calculated ages using the CRS model, versus mass thickness in SC-1 and SC-2 cores.

2019). As a first outcome, excess  $^{210}\text{Pb}$  total inventory ( $24 \pm 1 \text{ kBq.m}^{-2}$ ) was found to be nearly 4 folds higher in SC-2 core than in SC-1 core ( $6.0 \pm 0.4 \text{ kBq.m}^{-2}$ ). The corresponding annual fluxes of  $^{210}\text{Pb}$  to the sediment were estimated from the total inventories and found to be  $745 \pm 31$  and  $188 \pm 11 \text{ Bq.m}^{-2}.\text{y}^{-1}$  in SC-2 and SC-1, respectively. The values corresponding to SC-1 core, retrieved from the Sardinia Channel, were much closer to those found in the south-western Mediterranean Sea (Benmansour *et al.*, 2006). The lower  $^{210}\text{Pb}$  inventory and annual input onto the sediment of the Sardinia channel (SC-1 core) is, in great part, attributed to the low activities recorded in the upper layers compared to those of SC-2 core. On the other hand, as expected, the time-dependent sediment accumulation rates (SAR) provided by CRS model for both cores are quite different suggesting distinctive sedimentation regimes. Indeed, the vertical profiles of SAR exhibited different behavior in the two cores during the last century: an almost linear increment of the sedimentation rates upwards in SC-2 core, and episodes of acceleration, deceleration and even uniform accumulation rates in SC-1 core (Fig. 5). The mean SAR corresponding to the upper layers of the Strait of Sardinia (SC-1 core,  $0.05 \text{ g.cm}^{-2}.\text{y}^{-1}$ ) was distinctively lower than that of Sicily channel (SC-2

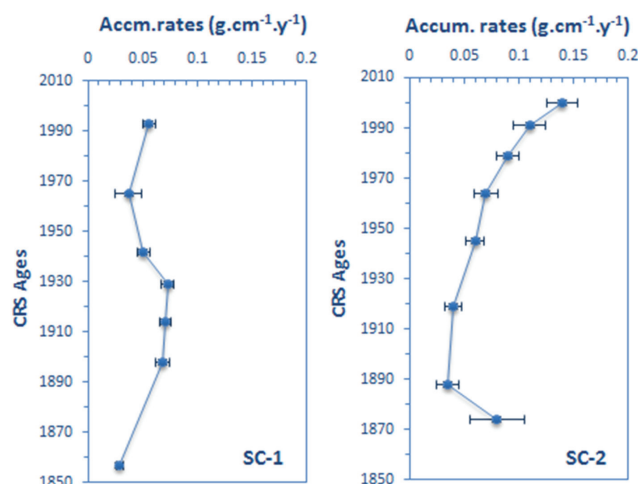


**Fig. 5:** Sediment accumulation rates versus CRS ages in SC-1 and SC-2 cores.

core,  $0.1 \text{ g.cm}^{-2}.\text{y}^{-1}$ ). A depth-averaged value of  $0.1 \text{ g.cm}^{-2}.\text{y}^{-1}$  was found in the Alboran Basin (Laissaoui *et al.*, 2008) from a core collected at 800 m depth. It is worth noting that the Strait of Sicily is the main connection be-

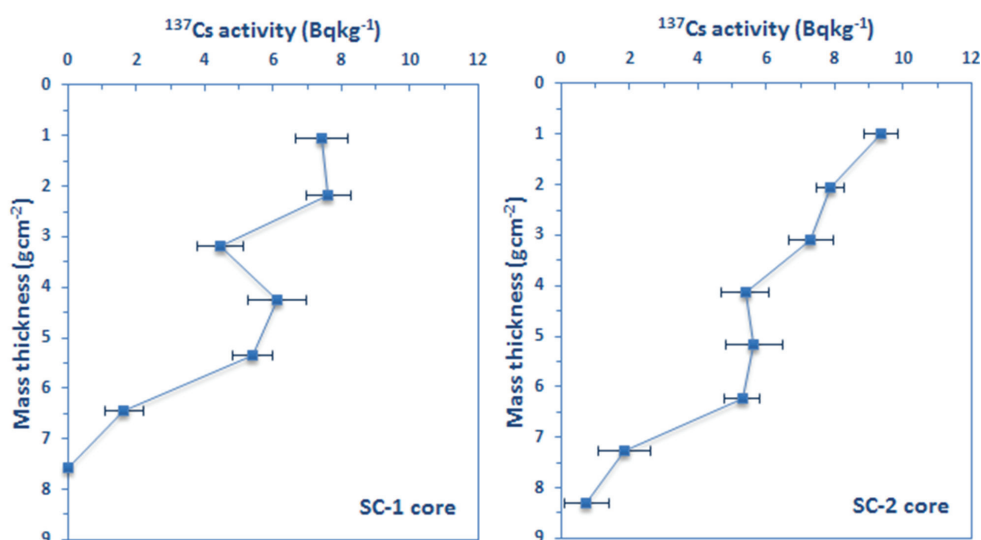


**Fig. 6:** Distribution of  $^{137}\text{Cs}$  concentrations versus mass thickness in SC-1 and SC-2 cores.

tween the eastern and western basin of the Mediterranean Sea. Thus, this area is characterized by large variability of mesoscale water circulation (Robinson *et al.*, 2001; El-Geziry & Bryden, 2010 ; Waldman *et al.*, 2018). Consequently, such differences in water dynamics in the two studied areas could yield to substantial variability in sedimentation processes. In addition, an inverse correlation between the depth-averaged accumulation rate and water depth was observed, being in agreement with earlier studies carried out in the northwestern Mediterranean Sea (Zuo *et al.*, 1997).

$^{137}\text{Cs}$  was measured in stratigraphic levels of both cores to validate the CRS chronologies. The corresponding profiles were plotted in Figure 6. The activities found are in the range of values found in the Western Mediterranean Sea and the inventories were  $450 \text{ Bq.m}^{-2}$  and  $355 \text{ Bq.m}^{-2}$  in the Sicily and Sardinia channel, respectively. These values lay within the range of inventories reported in previous studies, such as an inventory of  $284 \text{ Bq.m}^{-2}$  that was found in the Alboran Basin from a sediment core collected at 800 m water depth (Laissaoui *et al.*, 2008). The high  $^{137}\text{Cs}$  activity concentrations observed in the Sicily channel could be attributed to the influence of the Levantine Intermediate Waters (LIW) that carry higher  $^{137}\text{Cs}$  concentrations due to the Chernobyl accident (Lee *et al.*, 2006).

Cesium-137, being an anthropogenic radionuclide, has been widely used as independent tracer for validation of excess  $^{210}\text{Pb}$  derived ages (Lima *et al.*, 2005; Garcia-Orellana *et al.*, 2009), although some constraints on its use as time-marker in sediment dating have been reported in the scientific literature (Abril, 2004; Laissaoui *et al.*, 2008; Al-Mur *et al.*, 2017). According to the CRS model, the peak of maximum  $^{137}\text{Cs}$  concentration should be located at 1-2 cm and 3-4 cm depth in SC-1 and SC-2, respectively. The nonexistence of a well resolved peak in the  $^{137}\text{Cs}$  profiles is most probably due to post-depositional vertical migration. This downcore diffusion engendered a broadening effect which has resulted in detecting  $^{137}\text{Cs}$  in deeper layers corresponding to periods much earlier than the beginning of the atmospheric nuclear tests. This phenomenon has been previously reported in the sci-

entific literature (Oughton *et al.*, 1997; Foster *et al.* 2006; Fukushima *et al.*, 2017). It was also stated that diffusion could occur in both upward and downward directions, but the position of the maximum is not affected. In addition, due to the low sedimentation rate recorded in SC-1 core ( $0.4 \text{ mm.y}^{-1}$ ), the peak should have been obvious if depth resolution was higher. Indeed, the activity measured in 1 cm sediment thickness is the average value of the activities of many thin layers accumulated during many years (Omokheyeke *et al.*, 2014).

## Conclusion

From the two studied sediment cores collected from the Sardinia and Sicily channels, it was possible to contrast radionuclide levels, total inventories and sedimentation patterns in an area connecting the western and eastern basins of the Mediterranean Sea.

Two sedimentation regimes were identified,  $0.05$  and  $0.1 \text{ g.cm}^{-2}.\text{y}^{-1}$  in the Straits of Sardinia and Sicily, respectively, indicating substantial differences in sediment accumulation rates and historical patterns. The SAR vertical profiles showed an almost linear increment upwards in the Sicily strait, and episodes of acceleration, deceleration and even uniform sedimentation in the Sardinia channel. Excess  $^{210}\text{Pb}$  and  $^{137}\text{Cs}$  inventories and fluxes are inversely correlated with the water depths.

## Acknowledgements

This work was carried out in the framework of the IAEA International Atomic Energy Agency, Regional Project RAF/7/009 «Supporting an Integrated Approach for Marine Pollution Monitoring using Nuclear Analytical Techniques». The authors would like to thank the Moroccan authorities for hosting the fellowship «Marine Environment and Coastal Zone Management» at the CNESTEN National Center for Energy, Nuclear Science and Technology.

## References

- Abril, J.M., 2004. Constraints on the use of  $^{137}\text{Cs}$  as a time-marker to support CRS and SIT chronologies. *Environmental Pollution*, 129, (1), 31-37.
- Abril, J.M., 2003. A new theoretical treatment of compaction and the advective-diffusive processes in sediments: a reviewed basis for radiometric dating models. *Journal of Paleolimnology*, 30, (4), 363-370.
- Al-Mur, B.A., Quicksall, A.N., Kaste, J.M., 2017. Determination of sedimentation, diffusion, and mixing rates in coastal sediments of the eastern Red Sea via natural and anthropogenic fallout radionuclides. *Marine Pollution Bulletin*, 122, (1-2), 456-463.
- Arias-Ortiz, A., Masqué, P., Garcia-Orellana, J., Serrano O., Mazarrasa I. *et al.*, 2018. Reviews and syntheses:  $^{210}\text{Pb}$ -derived sediment and carbon accumulation rates in vegetated coastal ecosystems—setting the record straight. *Biogeosciences*, 15, 6791-6818.
- Benmansour, M., Nouira, A., Bouksirate, H., Benkdad, A., Ibn Majah, M., 2006. Use of fallout radionuclides to estimate short and long-term rates of soil erosion on agricultural lands in Morocco. In: Proceeding of 14th International Soil Conservation Organisation Conference, 14e19 May 2006, Marrakech, Morocco, Session Isotopes, 114 pp.
- Bonotto D.M., Garcia-Tenorio, R., 2019. Investigating the migration of pollutants at Barreiro area, Minas Gerais State, Brazil, by the  $^{210}\text{Pb}$  chronological method. *Journal of Geochemical Exploration*, 196, 219-234.
- Brenner, M., Schelske, C.L., Kenney, W.F., 2004. Inputs of dissolved and particulate  $^{226}\text{Ra}$  to lakes and implications for  $^{210}\text{Pb}$  dating recent sediments. *Journal of Paleolimnology*, 32, (1), 53-66.
- Bressac, M., Levy, I., Chamizo, E., La Rosa, J.J., Povinec, P.P. *et al.*, 2017. Temporal evolution of  $^{137}\text{Cs}$ ,  $^{237}\text{Np}$ , and  $^{239+240}\text{Pu}$  and estimated vertical  $^{239+240}\text{Pu}$  export in the northwestern Mediterranean Sea. *Science of The Total Environment*, 595, 178-190.
- Eleftheriou, G., Tsabaris, C., Papageorgiou, D.K. *et al.*, 2018. Radiometric dating of sediment cores from aquatic environments of north-east. *Mediterranean. Journal of Radioanalytical and Nuclear Chemistry*, 316, (2), 655-671.
- Fontela, M., Francés, G., Quintana, B., Álvarez-Fernández, M.J., Nombela, M.A. *et al.*, 2019. Dating the Anthropocene in deep-sea sediments: How much carbon is buried in the Irminger Basin?, *Global and Planetary Change*, 175, 92-102.
- Ebaid, Y., Khater, A., 2006. Determination of  $^{210}\text{Pb}$  in environmental samples. *Journal of Radioanalytical and Nuclear Chemistry*. *Journal of Radioanalytical and Nuclear Chemistry*, 270, (3), 609-619.
- El-Geziry, T.M., Bryden, I.G., 2010. The circulation pattern in the Mediterranean Sea: issues for modeller consideration. *Journal of Operational Oceanography*, 3, (2), 39-46.
- Foster, I.D.L., Mighall, T.M., Proffitt, H., Walling, D. E., Owens, P. N., 2006. Post-depositional  $^{137}\text{Cs}$  Mobility in the Sediments of Three Shallow Coastal Lagoons, SW England. *Journal of Paleolimnology*, 35 (4), 881-895.
- Fukushima, T., Komatsu, E., Arai, H., Kamiya, K., Onda, Y., 2017. Shifts of radiocesium vertical profiles in sediments and their modelling in Japanese lakes. *Science of The Total Environment*, 7, (615), 741-750.
- Garcia-Orellana, J., Pates, J.M., Masqué, P., Bruach, J.M., Sanchez-Cabeza, J.A., 2009. Distribution of artificial radionuclides in deep sediments of the Mediterranean Sea. *Science of The Total Environment*, 407, (2), 887-898.
- Garcia-Orellana, J., Sanchez-Cabeza, J.A., Masqué, P., Àvila, A., Costa, E., *et al.*, 2006. Atmospheric fluxes of  $^{210}\text{Pb}$  to the western Mediterranean Sea and the Saharan dust influence, *Journal of Geophysics. Research*, 111, (5).
- Haddad Kh., 2014. True coincidence summing correction determination for  $^{214}\text{Bi}$  principal gamma lines in NORM samples. *Journal of Radioanalytical Nuclear Chemistry*, 300, (2), 829-834.
- Hamilton, T.F., Smith, J.D., 1986. Improved alpha-energy resolution for the determination of polonium isotopes by alpha-spectrometry. *Applied Radiation and Isotopes*, 37, 628-630.
- Hurtado-Bermúdez, S., Jurado-González, J.A., Santos, J.L., Díaz-Amigo, C.F., Aparicio, I., *et al.*, 2018. Baseline activity concentration of  $^{210}\text{Po}$  and  $^{210}\text{Pb}$  and dose assessment in bivalve molluscs at the Andalusian coast. *Marine Pollution Bulletin*, 133, 711-716.
- Jia, J., Yang, Y., Cai, T., Gao, J., Xia, X., *et al.*, 2018. On the sediment age estimated by  $^{210}\text{Pb}$  dating: probably misleading “prolonging” and multiple-factor-caused “loss”. *Acta Oceanologica Sinica*, 37, (6), 30-39.
- Khater, A.E.M., Ebaid, Y.Y., 2008. A simplified gamma-ray self-attenuation correction in bulk samples. *Applied Radiation and Isotopes*, 66, (3), 407-413.
- Laissaoui, A., Benmansour, M., Ziad, N., Ibn Majah, M.J., Abril, M. *et al.*, 2008. Anthropogenic radionuclides in the water column and a sediment core from the Alboran Sea: application to radiometric dating and reconstruction of historical water column radionuclide concentrations. *Journal of Paleolimnology*, 40, 823-833.
- Lee, S.H., Mantoura, F.R., Povinec, P.P., Sanchez-Cabeza, J.A., Pontis, J.L. *et al.*, 2006. Distribution of anthropogenic radionuclides in the water column of the south-western Mediterranean Sea. *Radioactivity in the Environment*, 8, 137-147.
- Lima A.L., Hubeny J.B., Reddy, C.M., King, J.W., Huguen, K.A. *et al.*, 2005. High-resolution historical records from Pettaquamscutt River basin sediments:  $^{210}\text{Pb}$  and varve chronologies validate record of  $^{137}\text{Cs}$  released by the Chernobyl accident. *Geochimica et Cosmochimica Acta*, 69, (7), 1803-1812.
- Matthews, K.M., Kim, C.K., Martin, P., 2007. Determination of  $^{210}\text{Po}$  in environmental materials: a review of analytical methodology. *Applied Radiation Isotopes*, 65, 267-279.
- Mejjad, N., Laissaoui, A., El-Hammoumi, O., Benmansour, M., Benbrahim, S. *et al.* 2016. Sediment geochronology and geochemical behavior of major and rare earth elements in the Oualidia Lagoon in the western Morocco. *Journal of Radioanalytical and Nuclear Chemistry*, 309, (3), 1133-1143.
- Miralles, J., Radakovitch, O., Aloisi, J.-C., 2005.  $^{210}\text{Pb}$  sedimentation rates from the Northwestern Mediterranean margin. *Marine Geology*, 216, (3), 155-167.
- Omokheyke, O., Sikoki, F.D., Laissaoui, A., Akpuluma, D., Onyagbodor, P. *et al.*, 2014. Sediment geochronology and

- spatio-temporal and vertical distributions of radionuclides in the Upper Bonny Estuary (South Nigeria). *Geochronometria*, 41, (4), 369-376.
- Oughton, D.H., Børretzen, P., Salbu, B., Tronstad, E., 1997. Mobilisation of  $^{137}\text{Cs}$  and  $^{90}\text{Sr}$  from sediments: potential sources to arctic waters. *Science of The Total Environment*, 202, (1-3), 155-165.
- Piroddi, C., Coll, M., Lique, C., Macias, D., Greer, K., 2017. Historical changes of the Mediterranean Sea ecosystem: modelling the role and impact of primary productivity and fisheries changes over time. *Nature*, 7, scientific report, article number: 44491
- Robinson, A.R., Wayne, L., Alexander, T., Lascaratos, A., 2001. Mediterranean Sea Circulation. *Oceanography*, 27, 2575.
- Robinson, A.R., Leslie, W., Theoharis, A., Lascaratos, A., 2001. Mediterranean Sea Circulation. *Encyclopedia of Ocean Sciences*, 1689–1706. Academic Press Ltd., London.
- Sanchez-Cabeza, J.A., Masqué, P., Ani Ragolta, I., Merino, J., Frignani, M., 1999. Sediment accumulation rates in the southern Barcelona continental margin (NW Mediterranean Sea) derived from  $^{210}\text{Pb}$  and  $^{137}\text{Cs}$  chronology. *Progress in Oceanography*, 44, (1-3), 313-332.
- Waldman, R., Brüggemann, N., Bosse, A., Spall, M., Somot, S., & Sevault, F., 2018. Overturning the Mediterranean thermohaline circulation. *Geophysical Research Letters*, 45, 8407–8415.
- Zuo, Z., Eisma, D., Gieles, R., Beks, J., 1997. Accumulation rates and sediment deposition in the northwestern Mediterranean. *Deep Sea Research Part II: Topical Studies in Oceanography*, 44, (3-4), 597-609.